Optimized Texture Spectral Similarity Criteria

Michal Havlíček[1] and Michal Haindl[1,2(✉)]

[1] The Institute of Information Theory and Automation of the Czech Academy of Sciences, 182 08 Prague, Czechia
{havlimi2,haindl}@utia.cas.cz
[2] Faculty of Management, University of Economics, Jindřichův Hradec, Czechia
http://ro.utia.cas.cz/

Abstract. This paper introduces an accelerated algorithm for evaluating criteria for comparing the spectral similarity of color, Bidirectional Texture Functions (BTF), and hyperspectral textures. The criteria credibly compare texture pixels by simultaneously considering the pixels with similar values and their mutual ratios. Such a comparison can determine the optimal modeling or acquisition setup by comparing the original data with their synthetic simulations. Other applications of the criteria can be spectral-based texture retrieval or classification. Together with existing alternatives, the suggested methods were extensively tested and compared on a wide variety of color, BTF, and hyper-spectral textures. The methods' performance quality was examined in a long series of specially designed experiments where proposed ones outperform all tested alternatives.

Keywords: Texture spectral similarity criterion · Bidirectional texture function · Hyperspectral data · Texture modeling

1 Introduction

A fully automatic texture, or more generally image, quality assessment, i.e., mutual similarity evaluation of two or more of them, presents a fundamental but still unsolved complex problem. The validation of the state-of-the-art image and texture fidelity criteria on the web-based benchmark (http://tfa.utia.cas.cz) has demonstrated that none of the published criteria, e.g., CW-SSIM [26], STSIM-1, STSIM-2, STSIM-M [30], ζ [14] can be reliably used for this task [6]. Reliable criterion would support texture model development by comparing the original texture with a synthesized or reconstructed one to select optimal parameter settings of such a model. Such similarity metrics could also play an essential role in efficient content-based image retrieval, e.g., digital libraries or multimedia databases.

Methods based on various textural features developed and applied for texture categorization, such as Haralick's features [8], Run-Length features [2], Laws' filters [16], Gabor features [18], LBP [21], and many others cannot rank textures according to their visual similarity. These features are not descriptive, and thus they are helpful only for binary decisions: two mono-spectral textures are identical or not. Markovian textural features [7] are the rare exception. Many existing

© Springer Nature Switzerland AG 2021
K. Wojtkiewicz et al. (Eds.): ICCCI 2021, CCIS 1463, pp. 644–655, 2021.
https://doi.org/10.1007/978-3-030-88113-9_52

approaches are limited to mono-spectral images, which is a significant disadvantage as color is arguably the most significant visual feature.

The psychophysical evaluations [4], i.e., quality assessments performed by humans, currently represent the only reliable option. This approach requires a time-demanding experiment design setup, strictly controlled laboratory conditions, and representative sets of testers, i.e., sufficient numbers of individuals, ideally from the public, naive concerning the purpose and design of the experiment. Thus, such assessing is generally demanding, expensive, and unsuitable for daily routine practice, not feasible on demand. Moreover, human perception methods are inapplicable for hyper-spectral data due to human vision's limited tri-chromatic nature.

In this article, we assume that visual data be independent sets of pixels. The pixel values are compared as vectors while their position in the image is not considered. This restriction is called a spectral similarity comparison in the rest of the paper. It deals with the appearance and amount of pixels that occur in only one of the compared images and the ratio of pixels ratio appearing in both images to express their spectral composition difference.

The rest of the paper is organized as follows: Section 2 briefly presents published alternatives to solve image spectral similarity comparison, including some based on modifications of techniques developed for slightly different purposes. Section 3 explains in detail our approach and its optimization. Section 5 described the performed validation experiments and used test data. Section 6 shows the achieved results. Section 7 summarizes the paper with a discussion and compares our proposed criteria with the existing alternatives.

2 Related Work

Dealing with color images, i.e., containing three spectral channels, encourages using a three-dimensional (3-D) histogram or local histogram [28], which approximates the image color distribution. The most intuitive way is to compute the 3-D histogram difference (ΔH). Several other possibilities for 3-D histogram comparison have been suggested, such as the histogram intersection ($\cap H$) [24], the squared chord (d_{sc}) [13], and the Canberra metric (d_{can}) [13]. The information-theoretic measures can also be considered for evaluating the histogram difference, e.g., Jeffrey divergence (J) [22] or measure based on the χ^2 statistic (χ^2) [29].

Another possibility is represented by Earth Mover's Distance (EMD) or Wasserstein method [23] which can evaluate dissimilarity between two multi-dimensional distributions in some feature space. However, it turned out that the EMD is limited to tiny images, as demonstrated on average computing times of individual methods showed in Table 1.

The generalized colour moments (GCM) [19] and cosine distance (d_{cos}) [20, 29] suit well to the spectral similarity comparison problem. Different set-theoretic measures can serve as criteria as well, e.g., the Jaccard index (JI) [12] or the Sørensen-Dice index (SDI) [1].

Another alternative may be a modified criterion developed for texture comparison as the spectral similarity comparison might be considered an exceptional case of this task. It is possible to modify the structural similarity metric (SSIM) [25] by removing structure-related terms to obtain reduced SSIM [9].

The 3-D histogram-based criteria cannot be easily generalized to hyperspectral data, i.e., the data having more than three spectral channels, due to the impossibility of reliably estimating such histograms from limited sample data. GCM could be used for hyperspectral image comparison, but the number of multiplication terms to be integrated significantly increases, and so does the range of possible values of the criterion. Set-theoretic, $rSSIM$ and d_{cos} based criteria can handle the hyper-spectral data with no restriction. A more detailed overview can be found in [10].

3 Computation of MEMD

A new criterion for spectral similarity comparison was proposed - the mean exhaustive minimum distance (MEMD) [10]:

$$\downarrow \zeta(A,B) = \frac{1}{M} \sum_{(r_1,r_2)\in\langle A\rangle} \min_{(s_1,s_2)\in U} \left\{\rho\left(Y^A_{r_1,r_2,\bullet}, Y^B_{s_1,s_2,\bullet}\right)\right\} \qquad \geq 0 \ , \qquad (1)$$

where $Y^A_{r_1,r_2,\bullet}$ represents the pixel at location (r_1, r_2) in the image A, $\bullet$ denotes all the corresponding spectral indices, and similarly for $Y^B_{s_1,s_2,\bullet}$. Further, ρ is an arbitrary vector metric. U is the set of unprocessed pixel indices of B (explained in detail below), $M = \min\{\sharp\{A\}, \sharp\{B\}\}$, $\sharp\{A\}$ is the number of pixels in A, and similarly for $\sharp\{B\}$ and $\min\{\emptyset\} = 0$.

The term $\zeta(A,B)$ is evaluated using raster scanning of A. The algorithm examines the pixels of A, from the upper left corner. Each pixel searches for the index in the set U for which the corresponding pixel is the closest one, in the sense of the used metric ρ. U contains all spatial indices of the image B at the beginning of the process. When such a pixel is identified at $(s_1, s_2) \in U$, the distance between this pixel and the scanned one from A, measured by ρ, is added to the sum and the index (s_1, s_2) is removed from the set U. The algorithm proceeds to the right bottom of the image A and stops when either all pixels of A are examined, or U becomes an empty set.

The criterion $\zeta(A,B)$ is not symmetrical, but can be easily symmetrized as [10]: $\zeta_S(A,B) = \frac{1}{2}(\zeta(A,B) + \zeta(B,A))$ if needed. Another analytical properties of (1) are [10]: $\zeta(A,B) = 0 \leftrightarrow A = B$ (equality), $\zeta(A,A) = 0$ (reflexivity), $\zeta(A,B) \leq \zeta(A,B')$ for $B' \subset B$ (set cardinality dependence).

Two modifications of (1), which take into account color differences just noticeable by color psychometric methods in the CIE Lab color space [27], were suggested [10]:

$$\downarrow \zeta_2(A,B) = \frac{1}{M} \sum_{(r_1,r_2)\in\langle A\rangle} \kappa(r_1,r_2) \qquad \geq 0 \ ,$$

$$\kappa(r_1, r_2) = \begin{cases} 1, & \rho^* > 2.3, \\ 0, & otherwise, \end{cases}$$
$$\rho^* = \min_{(s_1,s_2)\in N} \left\{ \rho^{CIE} \left(Y^A_{r_1,r_2,\bullet}, Y^B_{s_1,s_2,\bullet} \right) \right\} \ , \tag{2}$$

where the threshold 2.3 was determined in [17] and ρ^{CIE} is the Euclidean distance from pixel $Y^A_{r_1,r_2,\bullet}$ to pixel $Y^B_{s_1,s_2,\bullet}$ in the CIE Lab color space. Finally, the last suggested criterion is the weighted average of the just-noticeable differences [10]:

$$\downarrow \zeta_3(A, B) = \frac{1}{M} \sum_{(r_1,r_2)\in A} \kappa(r_1, r_2)\, \rho^* \qquad \geq 0 \ . \tag{3}$$

The terms ζ_2 and ζ_3 are evaluated the same way as the term ζ. Notice that the proposed criterion ζ applies to any number of spectral bands, not only for the usual three spectral bands of the standard color images, while ζ_2 and ζ_3 are applicable for the images defined on CIE Lab color space.

4 Optimization

The criterion (1) and its modifications (2), (3) have been optimized to reduce time requirements without significantly increasing memory requirements while maintaining their quality. The pixels of the images to be compared are stored in the same ordered set in the optimized algorithm variant. Thus, each element of that set is assigned a variable identifying the pixel's source image. The data in the set are sorted using quicksort [11] sorting algorithm.

Table 1. The average evaluation time, on Pentium-2.8 GHz-equivalent CPU, depending on the size of compared images for individual criteria.

	8×8	16×16	32×32	64×64
ΔH, $\cap H$, d_{sc}, d_{can}, J, χ^2	0.7 s	0.7 s	0.7 s	0.7 s
EMD	1.8 ms	85.6 ms	5.7 s	7.6 min
ΔGCM^{111}_{00}	67.0 µs	0.1 ms	0.2 ms	0.5 ms
d_{cos}	32.0 µs	88.0 µs	93.0 µs	0.6 ms
JI , SDI	0.3 ms	4.0 ms	9.0 ms	48.0 ms
$rSSIM$	31.0 µs	0.1 ms	0.2 ms	1.4 ms
ζ	0.1 ms	2.0 ms	18.0 ms	0.2 s
$\zeta_{Optimized}$	39.0 µs	0.4 ms	1.2 ms	17.5 ms

Values of individual spectral channels of the given pixel form vector. The maximum metric applied on these vectors is used as an order relation. The rest of the method is formally the same, although the implementation is slightly different. The algorithm passes through the sorted set of pixels. For each pixel

belonging to the first compared image, the algorithm searches a pixel belonging to the other image so that their distance is minimal in the sense of the maximum metric. During the search in the set, we use advantageously the fact that the data are sorted. Suppose a situation in the distance of the compared pixels, i.e., the pixel from the first image and the candidate for the most similar pixel from the other image, is more distant than the previous candidate. In that case, the search can be terminated, and the distance of the compared pixel from the first image and the previous candidate can be indicated as the minimum one as illustrated in Fig. 1. This step leads to a significant acceleration of the entire algorithm as shown in Table 1 comparing the computational times for both variants of the algorithm and the compared alternative criteria.

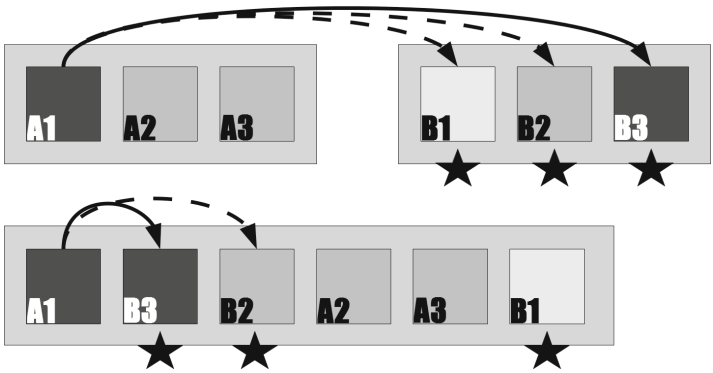

Fig. 1. The comparison of the original MEMD algorithm (upper scheme) with its optimized version (lower scheme). Comparing images A and B and their corresponding pixels A1, A1, A1 and B2, B2, B3, respectively. In the original version, there are three necessary comparisons (marked with arrows) of the pixel from the first image (A1) with the pixels from the second image B1, B2, B3 (marked with a star) to find the pixel from the second image (B3), which is the most similar to the scanned pixel (A1) from the first image (marked with solid line arrows). While there is only one necessary such comparison in the optimized version as the second pixel from the second image in the sorted set (B2) is less similar to the scanned pixel from the first image (A1) than the first pixel from the second image in the sorted set (B3), and there cannot exist a more similar one as the data are sorted.

5 Comparison

The proposed criteria (1)–(3) together with the previously published alternatives mentioned in Sect. 2 have been extensively tested on the experiments described in detail in Sect. 5.1 to investigate how the individual criteria are affected by the spectral composition changes in the compared images.

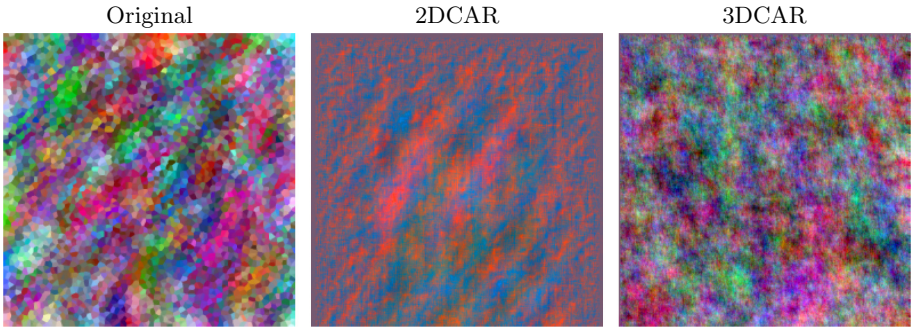

Fig. 2. Example of the use of the proposed criterion MEMD. The original image is compared with the images synthesized using 2D CAR [3] and 3D CAR [5] models, respectively. The values below individual images equal the difference between them and the original expressed by MEMD.

5.1 Controlled Degradation of the Test Data

A sequence of gradually degraded images is generated from the original test one. The original image serves as the first member of the sequence, i.e., $A_1^X = A$ and each member, except for the first one, is generated from its predecessor in the sequence as: $A_t^X = f_X\left(A_{t-1}^X\right), \quad t = 1, \ldots, l$, where l equals the length of the sequence and X is the label identifying the experiment (individual experiments described below). Further $Y_{r,t}^A$ denotes the multi-spectral pixel from the experimental image A_t^X at $r = [r_1, r_2, r_3]$ which is a multi-index with image row, column, and spectral components, respectively. X is the corresponding label of one of the following nine degradation experiments established for validation tests:

A - replacing pixel spectral intensities with the maximal value in the used colour space with the probability $p = \frac{1}{l}$
B - adding a constant $c = \frac{255}{l}$ to all pixel spectral intensities
C - adding a value $\frac{255}{l} \sin(\pi \frac{o}{l})$ depending on the order of the image in the sequence (o) to pixel spectral intensities
D - adding a constant $c = \frac{255}{l}$ to pixel spectral intensities and random mutual interchanging with probability $p = 0.5$ with 4-connected neighbourhood
E - adding a constant $c = \frac{255}{l}$ to pixel spectral intensities and randomly driven propagating with probability $p = 0.5$ with 8-connected neighbourhood
F - adding a value equals to the order of the image in the sequence (o) to pixel spectral intensities
G - adding a pseudo-random vector to each pixel
H - blurring the images using the convolution with the 3×3 Gaussian filter
I - adjusting pixel spectral intensities so as to approach average over spectral channels

More detailed description of the experiments including showed several examples of degraded images created during the experiments can be found in [10].

5.2 Evaluation Meta-criterion

The tested criteria are applied to quantifying spectral composition differences between the template image, i.e., the first member of the degradation sequence and the remaining members. As all those sequences are constructed so that monotone degradation of the original image is guaranteed, i.e., the similarity of the members of the sequence and the original image decreases with increasing order, and criterion should follow this trend.

The meta-criterion is the number of monotonicity violations of the criterion τ in the experiment X [10]:

$$\Xi^{X,\tau} = \sum_{i=1}^{l} \left[1 - \delta\left(o_i^X - o_i^{X,\tau}\right)\right] \quad , \tag{4}$$

where τ is a tested criterion, o_i^X is the rank of a degraded image and $o_i^{X,\tau}$ its corresponding correct ordering of the τ-criterion-based ranking, and δ is the Kronecker delta function.

5.3 Test Data

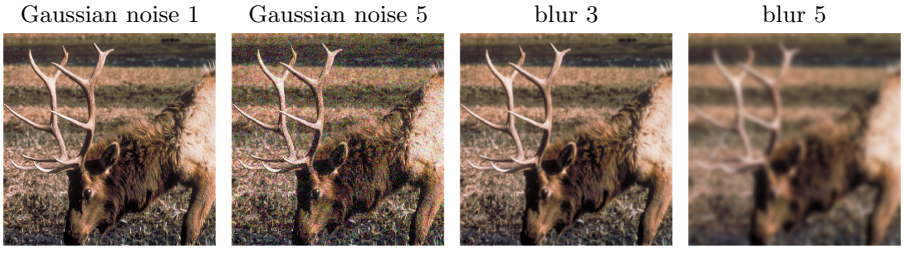

Fig. 3. Comparison between DMOS and MEMD criteria on the CSIQ image degradation examples.

Suggested criteria were validated and compared with the alternative measures on three types of visual data: color, BTF, and hyper-spectral textures, respectively. Two hundred fifty color textures, 200 BTF textures, and three hyper-spectral textures were used. Detailed information about used test data, including showed selected samples, can be found in [10]. The MEMD criterion was also compared

with the differential mean opinion score (DMOS) from the CSIQ database [15] images (Fig. 3). The Spearman rank correlation between MEMD and DMOS criteria values was always 1 for all compared results (Gaussian additive noise, blurring, contrast, JPEG 2000, JPEG). Hence it suggests MEMD's high correlation with the human quality ranking.

Table 2. The average strict monotonicity violation (in percent) for 250 test color texture sequences per experiment performed in the RGB color space, the average over all experiments, and the rank for the tested criteria.

	A	B	C	D	E	F	G	H	I	⊘	Rank
$rSSIM$	43	44	46	42	42	20	47	25	47	39	9
d_{cos}	29	44	45	31	31	19	47	47	47	38	8
d_{can}	0	34	29	40	40	12	17	20	31	25	7
SDI	16	10	23	9	9	4	28	24	26	17	6
JI	10	8	26	7	7	4	28	24	26	16	5
J	7	5	9	7	7	3	14	24	14	10	4
ΔH	0	3	5	3	3	1	13	16	8	6	3
$\cap H$	0	3	5	3	3	1	13	16	8	6	3
d_{sc}	0	3	5	4	4	1	14	17	9	6	3
χ^2	0	3	5	4	4	1	14	16	9	6	3
ΔGCM_{00}^{111}	0	0	0	0	0	0	11	9	3	3	2
ζ	0	0	0	0	0	0	0	2	0	0	1

6 Results

The achieved results for the optimized MEMD criterion (1) are summarized in Tables 2, 3 and 4 showing average strict monotonicity violation, i.e., fails, for individual criteria in individual experiments, in average and their rank, using color textures in RGB color space, color textures in CIE Lab color space, and hyper-spectral textures respectively. It is apparent that the proposed criteria (1)–(3) are universally the most reliable.

It holds for the original version of the algorithm and the optimized version, i.e., Tables 2, 3 and 4 as well. Both results are the same, Tables 2, 3 and 4 as well as the corresponding tables in [10], which proves that the presented optimization does not deteriorate the original criteria outstanding performance.

Table 3. The average strict monotony violation (in percent) for 250 test color texture sequences per experiment performed in the CIE Lab color space, the average over all experiments, and rank for tested criteria.

	A	B	C	D	E	F	G	H	I	⊘	Rank
$rSSIM$	46	46	45	46	46	21	46	40	46	42	9
d_{cos}	8	46	45	46	46	21	43	46	46	39	8
d_{can}	0	14	1	45	45	5	9	4	32	17	7
SDI	3	1	2	2	2	1	37	29	18	11	6
JI	1	1	2	1	1	1	37	29	16	10	5
J	1	1	2	1	1	1	25	25	12	7	4
ΔH	0	0	0	0	0	0	10	6	2	2	3
$\cap H$	0	0	0	0	0	0	10	6	2	2	3
d_{sc}	0	0	0	0	0	0	12	5	3	2	3
χ^2	0	0	0	0	0	0	11	5	3	2	3
ΔGCM_{00}^{111}	0	0	0	0	0	0	5	5	7	2	3
ζ_2	0	0	0	0	0	0	8	2	0	1	2
ζ_3	0	0	0	0	0	0	0	0	0	0	1
ζ	0	0	0	0	0	0	0	0	0	0	1

ΔGCM_{00}^{111}, ΔH, $\cap H$, d_{sc} and χ^2 are relatively reliable and thus applicable for spectral similarity comparison. The remaining criteria are significantly worse and thus unreliable. More detailed and commented results can be found in [10]. The results achieved using BTF textures are almost the same as those achieved using color textures as presented in [10]. Figure 2 illustrates the proposed MEMD criterion values for two different color texture model synthesis of the original texture.

Table 4. The average strict monotonicity violation (in percent) for 3 test hyper-spectral data sequences per experiment, average over all experiments and the rank for the tested criteria.

	A	B	C	D	E	F	G	H	I	⊘	Rank
$rSSIM$	36	38	46	28	28	18	47	25	47	37	4
d_{cos}	30	35	41	21	22	15	47	47	47	34	3
JI	0	3	4	4	3	2	24	24	3	7	2
SDI	0	2	2	3	3	1	25	25	5	7	2
ΔGCM_{00}^{111}	0	0	0	0	0	0	0	0	0	0	1
ζ	0	0	0	0	0	0	0	0	0	0	1

7 Conclusions

Accelerated variants of the criteria for comparing the spectral similarity of the color, BTF, and hyper-spectral textures were presented. Spectral similarity comparison represents a partial solution for general visual data quality assessment as individual pixels' positions are not considered. Despite this restriction, spectral similarity comparison criteria can assist in numerous texture-analytic or synthesis applications.

The performance quality of the optimized criteria was verified and demonstrated on the extensive series of 407,700 [10] specially designed monotonically image degrading experiments, which also served to compare with the existing alternative methods. These experiments proved that optimized versions of the criteria maintain the original ones' quality although they are significantly less time demanding, decreasing the average computing time to about 20% of the average computing time of the original algorithm. On the other hand, all three proposed criteria are still slightly more time-demanding than some alternative criteria except for EMD, which is both more time- and memory-demanding in such a practically unusable way spectral similarity comparison purposes.

Unlike many existing approaches, e.g., mentioned in Sect. 2, the MEMD criterion ζ (1) and its variants ζ_2 (2), ζ_3 (3) are not based on 3-D histograms, instead representing the estimate of the image spectral distribution, and requiring a sufficiently large data set, which is seldom available. Moreover, the criterion (1) has no limit on the number of spectral bands in the compared data. The proposed criteria can be exploited in simple spectral-based texture, image retrieval, or (un)supervised classification methods as demonstrated in [10].

The presented criteria propose a reliable, fully automatic alternative to psychophysical experiments, which are highly impractical due to their cost and strict design setup, condition control, human resources, and time. Additionally, psychophysical experiments are restricted to visualize maximally three-dimensional data due to the limited tri-chromatic nature of the human vision.

Acknowledgments. The Czech Science Foundation project GAČR 19-12340S supported this research.

References

1. Dice, L.R.: Measures of the amount of ecologic association between species. Ecology **26**(3), 297–302 (1945)
2. Galloway, M.M.: Texture analysis using gray level run lengths. Comput. Graphics Image Process. **4**(2), 172–179 (1975)
3. Haindl, M., Filip, J.: A fast probabilistic bidirectional texture function model. Lect. Notes Comput. Sci. **3212**, 298–305 (2004)
4. Haindl, M., Filip, J.: Visual Texture. Advances in Computer Vision and Pattern Recognition. Springer, London (2012). https://doi.org/10.1007/978-1-4471-4902-6
5. Haindl, M., Filip, J., Arnold, M.: BTF image space utmost compression and modelling method. In: Proceedings of the 17th IAPR International Conference on Pattern Recognition, vol. 3, pp. 194–197. IEEE Press (2004)

6. Haindl, M., Kudělka, M.J.: Texture fidelity benchmark. In: 2014 International Workshop on Computational Intelligence for Multimedia Understanding (IWCIM), pp. 1–5. IEEE (2014)
7. Haindl, M., Mikeš, S.: Unsupervised texture segmentation using multispectral modelling approach. In: 18th International Conference on Pattern Recognition (ICPR'06) vol. 2, pp. 203–206. IEEE (2006)
8. Haralick, R.M., Shanmugam, K., Dinstein, I.: Textural features for image classification. IEEE Trans. Syst. Man Cybern. **6**, 610–621 (1973)
9. Havlíček, M., Haindl M.: Texture spectral similarity criteria. In: Proceedings of the 4th CIE Expert Symposium on Colour and Visual Appearance, Commission Internationale de L'Eclairage CIE Central Bureau, pp. 147–154 (2016)
10. Havlíček, M., Haindl, M.: Texture spectral similarity criteria. IET Image Proc. **13**(11), 1998–2007 (2019)
11. Hoare, C.A.R.: Algorithm 64: quicksort. Commun. ACM **4**(7), 321 (1961)
12. Jaccard, P.: Etude comparative de la distribution florale dans une portion des Alpes et du Jura. Bull. Soc. Vaudoise Sci. Nat. **37**, 547–579 (1901)
13. Kokare, M., Chatterji, B., Biswas, P.: Comparison of similarity metrics for texture image retrieval. In: TENCON 2003, Conference on Convergent Technologies for Asia-Pacific Region, vol. 2, pp. 571–575 (2003)
14. Kudělka, M., Haindl, M.: Texture fidelity criterion. In: 2016 IEEE International Conference on Image Processing (ICIP), pp. 2062–2066. IEEE (2016)
15. Larson, E.C., Chandler, D.M.: Categorical image quality (CSIQ) database (2009). http://vision.okstate.edu/csiq
16. Laws, K.I.: Rapid texture identification. In: Image Processing for Missile Guidance, vol. 238, pp. 376–381. International Society for Optics and Photonics (1980)
17. Mahy, M., Eycken, L., Oosterlinck, A.: Evaluation of uniform color spaces developed after the adoption of CIELAB and CIELUV. Color. Res. Appl. **19**(2), 105–121 (1994)
18. Manjunath, B.S., Ma, W.Y.: Texture features for browsing and retrieval of image data. IEEE Trans. Pattern Anal. Mach. Intell. **18**(8), 837–842 (1996)
19. Mindru, F., Moons, T., Gool, L.V.: Color-based moment invariants for viewpoint and illumination independent recognition of planar color patterns. In: Singh, S. (ed.) International Conference on Advances in Pattern Recognition, pp. 113–122. Springer, London (1999). https://doi.org/10.1007/978-1-4471-0833-7_12
20. Moroney, N., Gottwals, M.M., Tasti, I.: Generating Color Similarity Measures, U.S. Patent No. 10,084,941. Washington, DC: U.S. Patent and Trademark Office (2018)
21. Ojala, T., Pietikäinen, M., Mäenpää, T.: Multiresolution gray-scale and rotation invariant texture classification with local binary patterns. IEEE Trans. Pattern Anal. Mach. Intell. **24**(7), 971–987 (2002)
22. Puzicha, J., Hofmann, T., Buhmann, J.M.: Non-parametric similarity measures for unsupervised texture segmentation and image retrieval. In: Proceedings of the IEEE International Conference on Computer Vision and Pattern Recognition, pp. 267–272. IEEE (1997)
23. Rubner, Y., Tomasi, C., Guibas, L.J.: The earth mover's distance as a metric for image retrieval. Int. J. Comput. Vision **40**(2), 99–121 (2000)
24. Swain, M.J., Ballard, D.H.: Color indexing. Int. J. Comput. Vision **7**(1), 11–32 (1991)
25. Wang, Z., Bovik, A.C., Sheikh, H.R., Simoncelli, E.P.: Image quality assessment: from error visibility to structural similarity. IEEE Trans. Image Process. **13**(4), 600–612 (2004)

26. Wang, Z., Simoncelli, E.P.: Translation insensitive image similarity in complex wavelet domain. In: Proceedings, (ICASSP 2005), IEEE International Conference on Acoustics, Speech, and Signal Processing, vol. 2, pp. 573–576. IEEE (2005)
27. Wyszecki, G., Stiles, W.S.: Color Science 8. Wiley, New York (1982)
28. Yuan, J., Wang, D., Cheriyadat, A.M.: Factorization-based texture segmentation. IEEE Trans. Image Process. **24**(11), 3488–3497 (2015)
29. Zhang, D., Lu, G.: Evaluation of similarity measurement for image retrieval. In: International Conference on Neural Networks and Signal Processing, Proceedings of the 2003, pp. 928–931. IEEE (2003)
30. Zujovic, J., Pappas, T.N., Neuhoff, D.L.: Structural texture similarity metrics for image analysis and retrieval. IEEE Trans. Image Process. **22**(7), 2545–2558 (2013)